

# Daphnetin Hydrazones – Synthesis and Screening of Anti-proliferative Potential Against Human Breast Cancer

Anees Pangal<sup>1,2</sup>, Inayatah Rasool<sup>1,2</sup>, Kounsar Sheikh<sup>1,2</sup>, Pranav Tambe<sup>1,2</sup>, Sudhir Bhagat<sup>1</sup>, Javed Mulla<sup>1</sup>, Aniket Phadatare<sup>1</sup>, Khursheed Ahmed<sup>1,2,\*</sup>

<sup>1</sup> Post-Graduate Department of Chemistry and Research Centre, Abeda Inamdar Senior College of Arts, Science and Commerce (Autonomous), Pune - 411001, India

<sup>2</sup> Advanced Scientific Research Laboratory, Azam Campus, Pune - 411001, India

\* Correspondence: [khursheedahmed@azamcampus.org](mailto:khursheedahmed@azamcampus.org);

Scopus Author ID7202086763

Received: 3.06.2024; Accepted: 6.10.2024; Published: 14.02.2025

**Abstract:** Six new hydrazones of 3-acetyldaphnetin were synthesized from 3-acetyldaphnetin (1) with different hydrazides and were tested for anti-proliferative activity against the human breast cancer cell line MCF-7 using an MTT assay. These hydrazones were computationally evaluated for ADMET and drug-likeness studies using online tools. Molecular docking methodology was applied to study the mode of interaction between the estrogen receptor (PDB ID: 3ERT), progesterone receptor (PDB ID: 3G8O), and human epidermal growth factor receptor 2 (HER2) (PDB ID: 3PP0). All the compounds showed promising anti-proliferative activity against the MCF-7 cell line, with IC<sub>50</sub> values ranging from 5.76 to 32.45  $\mu$ M. The ADMET properties of the compound 2c were determined, and this compound had accurate pharmacokinetic profiles. This hydrazone possesses good ADMET properties and showed drug-like properties with a strong affinity towards HER2, evidenced by its high binding energy compared to the other two targets.

**Keywords:** ADMET; breast cancer; coumarin; cytotoxicity; daphnetin; hydrazone; molecular docking.

© 2025 by the authors. This article is an open-access article distributed under the terms and conditions of the Creative Commons Attribution (CC BY) license (<https://creativecommons.org/licenses/by/4.0/>).

## 1. Introduction

Breast cancer, the second most common cancer in women, is one of the prime causes of female deaths [1]. Recently, a number of chemotherapy agents have been available for the treatment of breast cancer. However, due to the cytotoxicity and drug resistance, there is still a need to develop potent anti-breast cancer agents to overcome these problems [2,3]. The majority of breast cancers can be considered hormone-responsive, and about 75% of it is caused by the estrogen receptor (ER)2 [4]. The aromatase enzyme (ARO) is one of the enzymatic mechanisms that may regulate the increased estrogen levels found in breast cancer cells [5]. On the other hand, the most often over-expressed receptors in breast cancer cells are tyrosine kinase receptors (TKRs), e.g., the human epidermal growth factor receptor (EGFR/HER2) [6]. HER2 is expressed in many tissues, and its major role in these tissues is to aid in uncontrolled cell growth and tumorigenesis [7].

Over-expression of the HER2 gene occurs in approximately 15–30% of breast cancers, and it is now recognized that HER2 overexpression also occurs in other forms of cancers such as stomach, ovary, uterine serous endometrial carcinoma, colon, bladder, lung, uterine cervix,

head and neck, and esophagus [8]. Thus, targeting these receptors can be a promising way to develop novel anticancer drugs [9].

In the search for novel anticancer drugs, many coumarin derivatives derived from natural sources have been reported to exhibit potential anticancer activity [10]. Daphnetin (7,8-dihydroxycoumarin) is one of the simplest coumarins first isolated from plants of the genus *Daphne* [11]. Daphnetin possesses a number of biological activities [12] such as anti-inflammatory [13], antioxidant [14], analgesic [15], antipyretic [16], antimalarial [17], antibacterial [18], antiarthritic [19], neuroprotective [20], hepatoprotective [21], nephroprotective [22], immunosuppressive [23] and anticancer [24]. Similarly, hydrazones have also been reported to showcase a wide spectrum of biological activities such as anticancer, antimicrobial, anti-inflammatory, analgesic, antifungal, antitubercular, antiviral, anticonvulsant, and these activities are attributed to the distinctive structural features of hydrazones and azomethine group [25,26].

Additionally, the cheminformatic tools, predictions of ADMET, drug-likeness using Lipinski's rule of five, and molecular docking are useful applications for drug discovery [27]. ADMET, which constitutes the pharmacokinetic profile of a drug molecule, explains its absorption, distribution, metabolism, excretion, and toxicity and is essential for evaluating drug-like potential [28]. The ideal oral drug is rapidly and completely absorbed from the gastrointestinal tract, is distributed specifically to its site of action in the body, is metabolized in a way that does not instantly remove its activity, and is eliminated in a suitable manner without causing any harm. Therefore, pharmacokinetic properties (ADMET) are important determinants of the compound's success for human therapeutic use [29].

Considering the hybrid concept and the anticancer potential of coumarin scaffold, herein, we focused on the synthesis of new daphnetin hydrazones and evaluated their *in vitro* anti-proliferative potential against breast cancer cell line (MCF-7). The interaction of synthesized hydrazones and hormone receptors (ER, PR, and HER2) was assessed through docking studies, and their relative stabilities were evaluated using binding affinities. Additional data from computational studies is incorporated to evaluate the pharmacokinetic parameters associated with absorption, distribution, metabolism, elimination, and toxicity in the human body (ADMET), and the drug-like potential is subtly highlighted. Of the synthesized Daphnetin hydrazones, 2c was a more effective biological agent against MCF-7 targeting HER2.

## 2. Materials and Methods

### 2.1. Materials and methods.

The solvents used were purchased from commercial sources and dried further using standard protocols. 2,3,4-Trihydroxybenzaldehyde, benzoic acid hydrazide, salicylhydrazide, 3-hydroxybenzoic acid hydrazide, 4-hydroxybenzoic acid hydrazide, 2,4-dihydroxybenzoic acid hydrazide, and 3,4-dihydroxybenzoic acid hydrazide were obtained from Sigma-Aldrich chemicals, and ethyl acetate, piperidine, acetone, methanol, ethanol, and trifluoroacetic acid were obtained from SD-FCL and Loba Chemical Limited, Mumbai, India. Dulbecco's Modified Eagle Medium (DMEM) and fetal bovine serum (FBS) were purchased from Himedia, Mumbai. Thin-layer chromatography (TLC) was performed using commercially available Aluminium TLC plates coated with silica gel GF254. The developed plates were visualized by UV light and iodine vapors. The melting points of synthesized compounds were determined using an open capillary tube on a VEEGO melting point apparatus. All the

spectroscopic characterization data was obtained from CIF, Savitribai Phule Pune University, Pune. The 3-(4,5-dimethyl-2-thiazolyl)-2,5-diphenyl-2H-tetrazolium bromide (MTT) reagent was obtained from G-Biosciences, USA. The *in vitro* anticancer activities were carried out at the Advanced Scientific Research Laboratory, Abeda Inamdar Senior College, Pune.

## 2.2. General procedure.

A solution of 2,3,4-trihydroxy benzaldehyde (1.0g, 6.5 mmol) and ethyl acetoacetate (1.0ml, 8.5 mmol) in 10 ml methanol and 1-2 drops of piperidine was added. The reaction mixture was then heated to reflux for 5h. After cooling, the reaction mixture was poured slowly into a mixture of ice water (50ml) and stirred. The resultant suspension was filtered and dried. The crude compound was subsequently recrystallized from methanol to obtain compound 3-acetyl-7,8-dihydroxycoumarin or 3-acetyldaphnetin (**1**) [30]. To the solution of (**1**, 1 eq) and different benzoic acid hydrazides (1 eq) in ethanol, 5-6 drops of trifluoroacetic acid were added, and the mixture was stirred at room temperature till the completion of the reaction monitored with TLC, and then the reaction mixture was poured into the cold water. The solid obtained was filtered, washed with cold ethanol, and recrystallized from ethanol to obtain the target hydrazones (**2a-2f**) (Figure 1).

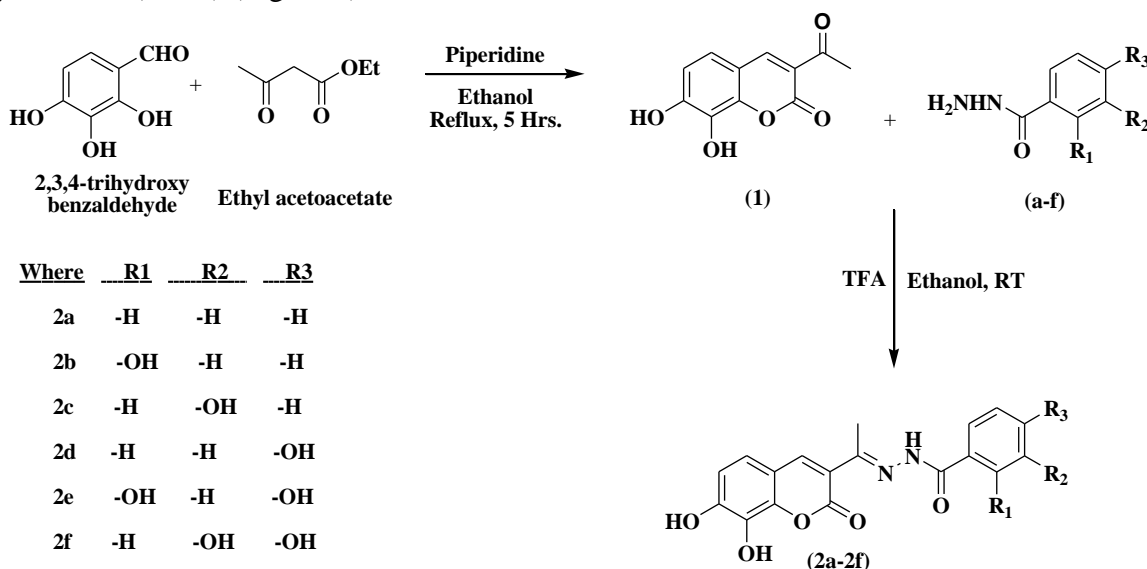


**Figure 1.** Synthesis of new Daphentin hydrazones (**2a-2f**).

The detailed physical properties and spectral characterization data are given below:

**(11E)-N'-(1-(7,8-dihydroxy-2-oxo-2H-chromen-3-yl)ethylidene)benzohydrazide(2a):** Pale yellow solid, 242-244°C, FTIR (cm<sup>-1</sup>): 3509.81 (-OH), 3286.11 (-NH), 1631.48 (C=O), 1592.91 (C=N), 1349.93 (Aromatic region), <sup>1</sup>HNMR (500, DMSO) δ 10.76 (s, 1H), 7.88 (d, 1H), 7.8 (d, 2H), 7.5 (m, 3H), 7.1 (dd 1H), 6.86 ((d, 1H), 2.55 (s, 3H). HRMS (ESI<sup>+</sup>): C<sub>18</sub>H<sub>14</sub>N<sub>2</sub>O<sub>5</sub>: 339.09.

**(11E)-2-hydroxy-N'-(1-(7,8-dihydroxy-2-oxo-2H-chromen-3-yl)ethylidene)benzohydrazide hydrate (2b):** Pale yellow solid, 238-240°C, FTIR (cm<sup>-1</sup>): 3544.52 (OH), 3228.25 (NH), 1631 (C=O), 1608.34 (C=N), 1346.07-1384.64 (Aromatic region), 1253.50 (C-O-C). <sup>1</sup>HNMR (500, DMSO) δ: 11.41 (s, 1H), 8.54 (s, 1H), 8.16(s, 1H), 7.98 (d, J = 7.3Hz, 1H), 7.46-7.37 (m, 1H), 7.22 ((d, J = 7.3 Hz, 1H), 6.98 (m, 3H), 2.55 (s, 3H). HRMS (ESI<sup>+</sup>): C<sub>18</sub>H<sub>14</sub>N<sub>2</sub>O<sub>6</sub>: 355.09.

**(11E)-3-hydroxy-N'-(1-(7,8-dihydroxy-2-oxo-2H-chromen-3-yl)ethylidene)benzohydrazide (2c):** Yellow solid, 244-246°C, FTIR (cm<sup>-1</sup>): 3575.38 (OH),

3316 (NH), 1592.91 (C=N), 1349.93-1380.78 (Aromatic region), 1245.79 (C-O-C), <sup>1</sup>HNMR (500, DMSO) δ: 10.67 (s, 1H), 10.37 (s, 1H), 9.7 (s, 2H), 8.0 (d, 1H), 7.3 (dd, 1H), 7.0 (d, 1H), 6.9 (s, 1H), 6.8 (dd, 1H), 2.55 (s, 3H), HRMS (ESI<sup>+</sup>): C<sub>18</sub>H<sub>14</sub>N<sub>2</sub>O<sub>6</sub>: 355.09.

**(11E)-4-hydroxy-N'-(1-(7,8-dihydroxy-2-oxo-2H-chromen-3-yl)ethylidene)benzohydrazide (2d):** Yellow solid, 248-250°C, FTIR (cm<sup>-1</sup>): 3594.66 (OH), 3278 (NH), 1623.77 (C=O), 1581 (C=N), 1349.93-1380.78 (Aromatic region), 1245.79 (C-O-C), <sup>1</sup>HNMR (500, DMSO) δ: 10.43 (s, 1H), 10.07 (s, 2H), 8.07 (d, 1H), 7.78 (dd, 1H), 7.1 (d, 1H), 6.8 (dd, 2H), 2.55 (s, 3H). HRMS (ESI<sup>+</sup>): C<sub>18</sub>H<sub>14</sub>N<sub>2</sub>O<sub>6</sub>: 355.09.

**(11E)-2,4-dihydroxy-N'-(1-(7,8-dihydroxy-2-oxo-2H-chromen-3-yl)ethylidene)benzohydrazide (2e):** Pale yellow solid, 246-248°C, FTIR (cm<sup>-1</sup>): 3559.95 (OH), 3309.25 (NH), 1631.48 (C=O), 1585.20 (C=N), 1349.93-1384.64 (Aromatic region), <sup>1</sup>HNMR (500, DMSO) δ: 11.41 (s, 1H), 7.8 (d, 1H), 7.3 (d, 2H), 7.1 (dd, J = 7.1, 1H), 6.8 (d, 1H), 6.2 (m, 2H), 2.55 (s, 3H), HRMS (ESI<sup>+</sup>): C<sub>18</sub>H<sub>14</sub>O<sub>7</sub>N<sub>2</sub>: 371.08.

**(11E)-3,4-dihydroxy-N'-(1-(7,8-dihydroxy-2-oxo-2H-chromen-3-yl)ethylidene)benzohydrazide (2f):** Yellow solid, 238-240°C, FTIR (cm<sup>-1</sup>): 3556.09 (OH), 3270.68 (NH), 1581.34 (C=N), 1346.07 (Aromatic region), <sup>1</sup>HNMR (500, DMSO) δ: 10.43 (s, 1H), 9.4 (s, 2H), 8.5 (d, 1H), 7.3 (dd, 1H), 6.7 (d, 1H), 6.8 (m, 2H), 2.55 (s, 3H). HRMS (ESI<sup>+</sup>): C<sub>18</sub>H<sub>14</sub>O<sub>7</sub>N<sub>2</sub>: 371.08.

### 2.3. *In vitro* anti-proliferative activity (MTT assay).

Compounds' *in vitro* anti-proliferative activity was evaluated against a human breast cancer cell line (MCF-7) using MTT assay protocol [31]. Adriamycin (ADR) was used in this test as a positive control. The tested cell lines were purchased from The National Centre for Cell Science (NCCS), Pune, and harvested on DMEM supplemented with 10% FBS and L-Glutamine 0.2 %. in a humidified 5% (v/v) CO<sub>2</sub> atmosphere at 37°C. Then, 1x10<sup>6</sup> cells per well from the cancer cell lines were seeded into each well. After 24 hours, the medium was replaced with fresh medium containing different dilutions of the compounds prepared using DMEM. After 48 hours of treatment, 5% MTT solution (100ul) was added and incubated further for 4 hours. MTT formazan crystals formed by metabolically viable cells were dissolved in DMSO (50ul). After 10-20 minutes, absorbance was recorded at 570 nm using Readwell Touch Automatic Elisa Plate Reader (Robonik India Private Limited). The metabolic viability of different cancer cell lines treated with test compounds was compared to untreated cells (taken as 100% viable). All the experiments were performed in triplicates, and the percentage growth was calculated using the formula:

$$\text{Percent Growth Inhibition} = \frac{T_i}{C} \times 100 \quad (1)$$

Where T<sub>i</sub> = growth of the microorganisms in the presence of the drug and C = Control growth.

### 2.4. ADMET, physicochemical and drug-like properties.

The ADMET properties were evaluated by uploading the SMILES format of the designed molecules on the pKCSM web server (<https://biosig.lab.uq.edu.au/pkcsml/prediction>). Specific ADMET parameters like gastrointestinal (GI) absorption, blood-brain barrier (BBB) permeability, CYP2D6 and CYP3A4 substrates and inhibitors, human skin permeability coefficients (log K<sub>p</sub>), Caco-2 permeability, the volume of distribution at steady state (VD<sub>ss</sub>), CNS permeability, total clearance, AMES toxicity, LD50 and a certain type of toxicities, skin

sensitization, etc. were assessed. Physicochemical and drug-like properties were evaluated using SwissADME (<http://www.swissadme.ch/>), a web-based platform that lets users upload or draw their target compounds with structure or SMILES code. This tool supplies many parameters, such as lipophilicity (XLOGP3) and drug-likeness rules [32].

### 2.5. Molecular docking.

CB-Dock2 is an improved version of the protein-ligand blind docking tool. It inherits the curvature-based cavity detection procedure and the AutoDockVina-based molecular docking procedures. To understand the probable mechanism of action and the binding affinities of the synthesized azo-coumarin derivatives, molecular docking studies of the most potent compound (**2c**) were carried out at active sites of three proteins viz. estrogen receptor (PDB Id: 3ERT), Progesterone Receptor (PDB Id: 3G8O), and Human epidermal growth factor receptor 2 (PDB Id: 3PP0) using the online molecular docking platform CB-Dock2 (<https://cadd.labshare.cn/cb-dock2>). The PDB files were downloaded from Protein Data Bank, RSCB PDB (<http://www.rscb.org>). Subsequently, the docking results were saved as PDB files and processed to observe the interactions in Discovery Studio software, following literature guidelines [33].

## 3. Results and Discussion

### 3.1. Chemistry.

The target compounds (**2a-2f**) were successfully obtained according to the two-step synthetic strategy outlined in Figure 1. Initially, 2,3,4-trihydroxy benzaldehyde and its ethyl acetoacetate underwent Knoevenagel condensation in the presence of piperidine to yield 3-acetyl-7,8-dihydroxycoumarin (3-acetyldaphnetin) (**1**). Subsequently, the coumarin (**1**) obtained in the first step was readily converted into the corresponding hydrazones by reacting them with different benzhydrazides in the presence of trifluoroacetic acid as a catalyst. The yields of the **2a-2f** target compounds varied from moderate to good. The structure and purity of final compounds were confirmed with IR, <sup>1</sup>HNMR, and HRMS data. The synthesized analogs' HRMS (ESI) spectra exhibited major peaks corresponding to the expected M+1 fragment at 339.09, 355.09, 355.09, 355.09, 371.08, and 371.08, respectively. The IR and NMR spectra displayed characteristic peaks for the functional groups present in the structures.

### 3.2. Anti-proliferative activity.

The *in vitro* anti-proliferative activity of compounds (**2a-2f**) was evaluated in the human breast cancer cell line, MCF-7, using different concentrations (100, 50, 25, 12.5, 6.25, and 3.125  $\mu$ M) of test compounds. The cells were treated for 48 hours, and cell viability was calculated. Adriamycin was used as a reference drug. The dose-response relationship revealed a dose-dependent decrease in cell viability upon increasing the concentration of the tested compounds. The growth curve for the MCF-7 cancer cell line after 48 hours was plotted to illustrate the relationship between cell growth and the drug concentration (Figure 2). Most of the tested compounds exhibited notable anti-proliferative activity for MCF-7 cells. All tested compounds (**2a-2f**) showed good to moderate activity compared to the standard control (Adriamycin).



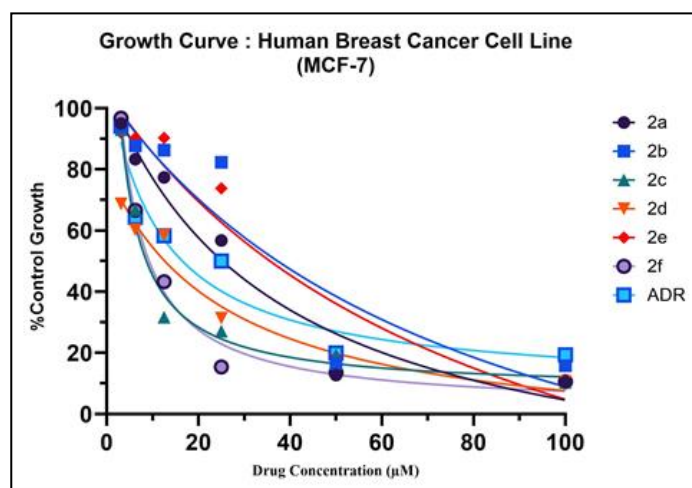


**Figure 2.** Growth curve: human breast cancer cell line (MCF-7).

The anti-proliferative effects of hydrazones were assessed using their  $IC_{50}$  values compared to the  $IC_{50}$  values of a standard drug (Table 1). All the tested compounds showed significant cytotoxicity against the MCF-7 cancer cell line, with  $IC_{50}$  values in the range of 5.76 – 32.45  $\mu$ M. Among the tested compounds, compounds **2c** and **2f** displayed the most potent inhibitory activity on MCF-7 cancer cell lines, with  $IC_{50}$  values of 5.76 and 6.98  $\mu$ M, respectively, comparable with the reference drug. The observed activity may be attributed to the presence of different functional groups in the structures of compounds **2a-2f**. Compounds with substituted phenyl rings exhibited higher activity compared to compound **2a**, which has no substituent on the phenyl ring of hydrazide. In contrast, hydrazones **2b**, **2d**, and **2e** exhibited moderate activity, with the hydroxy group substituted at the 2- or 4-position of the benzoic acid ring. From the results obtained, it can be concluded that the substitution at the 3-position of the benzoic acid ring, as in **2c**, is necessary for the enhanced activity[34].

**Table 1.**  $IC_{50}$  values of new Daphnetin hydrazones.

Hydrazones	$IC_{50}$ values ( $\mu$ M)
2a	$27.57 \pm 4.22$
2b	$31.46 \pm 4.12$
2c	$5.76 \pm 3.6$
2d	$21.54 \pm 2.6$
2e	$32.45 \pm 0.53$
2f	$6.98 \pm 2.4$
ADR	$1.30 \pm 3.81$

### 3.3. ADMET, Physicochemical and drug-like properties.

Encouraged by the significant anti-proliferative activity of **2c**, we assessed its suitability for further studies and development by predicting its ADMET and drug-likeness [35]. The ADMET properties of **2c** were assessed using pkCSM online tool, focusing on parameters such as water solubility, Caco-2 permeability, gastrointestinal absorption, skin permeability, VDss (human), CNS permeabilities, and BBB permeability. **2c** exhibited a gastrointestinal absorption rate of 72.27% and demonstrated good water solubility. It also showed a high Caco-2 permeability value of 0.986. However, it was predicted to have poor BBB permeability. The lack of inhibition of CYP2D6 and CYP3A4 suggests that **2c** will not interfere with the metabolism of xenobiotics in the body.

Additionally, it exhibited a favorable value for total clearance, contributing to its potential bioavailability. However, the hydrazone showed hepatotoxicity and was not skin-

sensitive. Furthermore, all these hydrazones act as non-carcinogenic, which is depicted by a negative AMES toxicity test. Thus, the overall result of ADMET studies uncovers good pharmacokinetic properties and ensures optimum oral bioavailability.

The physicochemical properties provide a comprehensive description of derivative structures, including molecular weight (MW), molar refractivity (MR), topological polar surface area (TPSA), number of rotatable bonds, heavy atoms, and hydrogen bond acceptors and donors. The physicochemical properties of **2c** were predicted using the SwissADME web server, focusing on specific parameters related to drug-likeness. The bioavailability properties of the analog are within a range that suggests oral bioavailability and makes them excellent drug candidates. The bioavailability predictions of the compounds displayed a rapid evaluation of drug-likeness. There are five different rule-based filters that are used to predict whether the chemical compounds can act as drugs. Compound **2c** did not violate the Lipinski, Ghose, Veber, and Muegge rules but violated the Egan rule due to higher TPSA value. The results of drug-likeness evaluation for analogs are presented in Table 2, providing insight into their suitability as drug candidates. Overall, **2c** exhibits desirable drug-like features while demonstrating significant anti-proliferative activity.

**Table 2.** ADMET, Physicochemical and drug-like properties of hydrazone **2c**.

ADMET properties of <b>2c</b> calculated from pkCSM			Physicochemical properties of <b>2c</b>	
Property	Model name	<b>2c</b>	Properties	<b>2c</b>
Absorption	Water solubility	-3.121	MW (g/mol)	354.31
	Caco-2 permeability	0.986	Heavy atoms	26
	Intestinal absorption (human)	72.279	Arom. heavy atoms	16
	Skin Permeability	-2.754	Rotatable bonds	4
Distribution	VDss (human)	0.155	H-Bond acceptors	7
	Fraction unbound (human)	0.084	H-Bond donors	4
	BBB permeability	-1.146	Molar Refractivity	94.53
	CNS permeability	-2.533	TPSA (Å <sup>2</sup> )	132.36
Metabolism	CYP2D6 inhibitor	No	Log S (ESOL)	-3.60
	CYP3A4 inhibitor	No	XLOGP3	2.18
Excretion	Total Clearance	0.533		
Toxicity	Max. tolerated dose (human)	0.384	Drug Likeness evaluation of <b>2c</b>	
	Oral Rat Acute Toxicity (LD50)	1.849	Rule	violations
	Oral Rat Chronic Toxicity	2.106	Lipinski	0
	Minnow toxicity	0.702	Ghose	0
	Hepatotoxicity	Yes	Veber	0
	Skin Sensitization	No	Egan	1
	AMES toxicity	No	Muegge	0

### 3.4. Molecular docking.

Understanding the prediction of interactions between proteins and small molecules is essential for identifying various biological processes, advancing drug development, and elucidating protein functions. A powerful approach for this purpose is protein-ligand blind docking, which identifies protein binding regions and predicts a molecule's binding pose. The MCF-7 cell line, known for its over-expression of ER, PR, and HER2, exhibited a significant decrease in the proliferation upon treatment with **2c** in MTT Assay. Molecular docking with ER (PDB: 3ERT), PR (PDB: 3G8O), and HER2 (PDB: 3PP0) revealed that the synthesized compounds exhibited good binding interactions with amino acid residues in the active site, as shown in Figure 3.

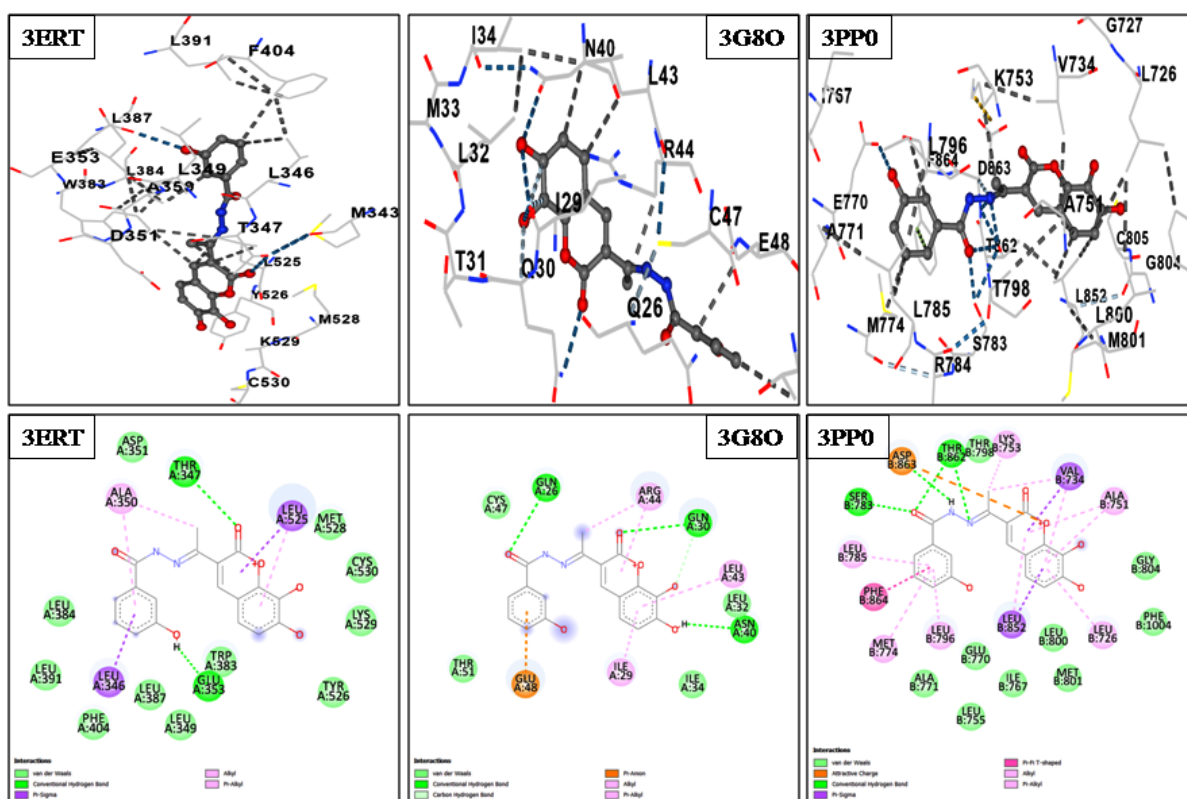


**Figure 3.** 3D and 2D representation for binding interactions of **2c** against human Estrogen receptor (PDB: 3ERT), Progesterone receptor (PDB: 3G8O) and HER2 receptor (PDB: 3PP0).

The estimated free binding energy for derivative **2c** with proteins (3ERT), (3G8O), and HER2 were -8.6 kcal/mol, -7.4 kcal/mol, and -11 kcal/mol, respectively, indicating favorable binding within the active site pocket of each protein. Furthermore, hydrazone **2c** exhibited greater selectivity towards HER2 protein, as evidenced by its higher binding energy than the other two targets. However, while the binding interactions observed during *in silico* investigations are promising, further *in vitro* investigations are needed to confirm these findings.

#### 4. Conclusions

In the present study, we have successfully synthesized the biologically active daphnetinhydrazones (**2a-2f**), with structural elucidation performed using FT-IR, <sup>1</sup>H-NMR, and HRMS techniques. During the anti-proliferative evaluation, the hydrazone **2c** and **2f** demonstrated noteworthy anti-proliferative potential against the MCF-7 cancer cell line. These hydrazones were computationally evaluated for ADMET, physicochemical, and drug-like properties, suggesting their potential as oral drugs with good pharmacokinetic profiles. Further, the hydrazone **2c** was subjected to molecular docking with ER (PDB: 3ERT), PR (PDB: 3G8O), and HER2 (PDB: 3PP0), and results showed that the compound showed good binding interactions with amino acid residues in the active site of these proteins. Among these three proteins, hydrazone **2c** showed a strong affinity towards HER2, as evidenced by its high binding energy compared to the other two targets. These obtained results can be accounted for by the presence of different groups in the molecular structure, especially OH, which is accountable for the interaction with the active site of the target protein. However, further *in vitro* and *in vivo* studies are required to confirm the findings of the chemoinformatics



investigation. These preliminary results may contribute to developing lead structures with selective anti-proliferative potential against breast cancer.

## Funding

This research was funded by the Department of Science and Technology, Govt. of India, for providing financial assistance under DST-FIST (0 Level) to Abeda Inamdar Senior College, Pune, vide letter number SR/FST/COLLEGE-277/2018 dated 20th December 2018.

## Acknowledgments

We are grateful to Dr. P. A. Inamdar, the President of MCE Society, Pune, and the principal of Abeda Inamdar Senior College, Pune, for providing the lab facilities and financial assistance.

## Conflicts of Interest

The authors declare no conflict of interest.

## References

1. Mehrotra, R.; Yadav, K. Breast cancer in India: Present scenario and the challenges ahead. *World J. Clin. Oncol.* **2022**, *13*, 209-218, <https://doi.org/10.5306/wjco.v13.i3.209>.
2. Kunštič, T.T.; Debeljak, N.; Tacer, K.F. Heterogeneity in hormone-dependent breast cancer and therapy: Steroid hormones, HER2, melanoma antigens, and cannabinoid receptors. *Adv. Cancer Biol. - Metastasis* **2023**, *7*, 100086, <https://doi.org/10.1016/j.adcanc.2022.100086>.
3. Khalaf, W.Y.; Elias, R.S.; Raheem, L.A. Design, synthesis and molecular docking study of coumarin pyrazoline derivatives against MCF-7 breast cancer cell line. *Pharmacia* **2023**, *70*, 1487-1492, <https://doi.org/10.3897/pharmacia.70.e108670>.
4. Murphy, C.G.; Dickler, M.N. Endocrine resistance in hormone-responsive breast cancer: mechanisms and therapeutic strategies. *Endocrine-Related Cancer* **2016**, *23*, R337-R352, <https://doi.org/10.1530/erc-16-0121>.
5. Franik, S.; Eltrop, S.M.; Kremer, J.A.M.; Kiesel, L.; Farquhar, C. Aromatase inhibitors (letrozole) for subfertile women with polycystic ovary syndrome. *Cochrane Database Syst. Rev.* **2018**, *5*, <https://doi.org/10.1002/14651858.cd010287.pub3>.
6. Nuciforo, P.; Radosevic-Robin, N.; Ng, T.; Scaltriti, M. Quantification of HER family receptors in breast cancer. *Breast Cancer Res.* **2015**, *17*, 53, <https://doi.org/10.1186/s13058-015-0561-8>.
7. Olayioye, M.A. Intracellular signaling pathways of ErbB2/HER-2 and family members. *Breast Cancer Res.* **2001**, *3*, 385-389, <https://doi.org/10.1186%2Fbcr327>.
8. Iqbal, N.; Iqbal, N. Human Epidermal Growth Factor Receptor 2 (HER2) in Cancers: Overexpression and Therapeutic Implications. *Mol. Biol. Int.* **2014**, *2014*, 852748, <https://doi.org/10.1155/2014/852748>.
9. Miziak, P.; Baran, M.; Błaszczak, E.; Przybyszewska-Podstawka, A.; Kałafut, J.; Smok-Kalwat, J.; Dmoszyńska-Graniczka, M.; Kielbus, M.; Stepulak, A. Estrogen Receptor Signaling in Breast Cancer. *Cancers* **2023**, *15*, 4689, <https://doi.org/10.3390/cancers15194689>.
10. Koley, M.; Han, J.; Soloshonok, V.A.; Mojumder, S.; Javahershenas, R.; Makarem, A. Latest developments in coumarin-based anticancer agents: mechanism of action and structure–activity relationship studies. *RSC Med. Chem.* **2024**, *15*, 10-54, <https://doi.org/10.1039/D3MD00511A>.
11. Moshiaashvili, G.; Tabatadze, N.; Mshvildadze, V. The genus Daphne: A review of its traditional uses, phytochemistry and pharmacology. *Fitoterapia* **2020**, *143*, 104540, <https://doi.org/10.1016/j.fitote.2020.104540>.
12. Javed, M.; Saleem, A.; Xaveria, A.; Akhtar, M.F. Daphnetin: A bioactive natural coumarin with diverse therapeutic potentials. *Front Pharmacol.* **2022**, *13*, 993562, <https://doi.org/10.3389/fphar.2022.993562>.
13. Yu, W.-w.; Lu, Z.; Zhang, H.; Kang, Y.-h.; Mao, Y.; Wang, H.-h.; Ge, W.-h.; Shi, L.-y. Anti-inflammatory and Protective Properties of Daphnetin in Endotoxin-Induced Lung Injury. *J. Agric. Food Chem.* **2014**, *62*, 12315-12325, <https://doi.org/10.1021/jf503667v>.

14. Xia, Y.; Chen, C.; Liu, Y.; Ge, G.; Dou, T.; Wang, P. Synthesis and Structure-Activity Relationship of Daphnetin Derivatives as Potent Antioxidant Agents. *Molecules* **2018**, *23*, 2476, <https://doi.org/10.3390/molecules23102476>.
15. Zhang, T.; Liang, W.; Ou, W.; Zhang, M.; Cui, S.; Zhang, S. Daphnetin alleviates neuropathic pain in chronic constrictive injury rats *via* regulating the NF- $\kappa$ B dependent CXCL1/CXCR2 signaling pathway. *Pharm. Biol.* **2023**, *61*, 746-754, <https://doi.org/10.1080/13880209.2023.2198560>.
16. He, Z.; Liu, J.; Liu, Y. Daphnetin attenuates intestinal inflammation, oxidative stress, and apoptosis in ulcerative colitis *via* inhibiting REG3A-dependent JAK2/STAT3 signaling pathway. *Environ Toxicol.* **2023**, *38*, 2132-2142, <https://doi.org/10.1002/tox.23837>.
17. Yang, Y.-Z.; Ranz, A.; Pan, H.-Z.; Zhang, Z.-N.; Lin, X.-B.; Meshnick, S.R. Daphnetin: a novel antimalarial agent with *in vitro* and *in vivo* activity. *Am. J. Trop. Med. Hyg.* **1992**, *46*, 15-20, <https://doi.org/10.4269/ajtmh.1992.46.15>.
18. Cottigli, F.; Loy, G.; Garau, D.; Floris, C.; Caus, M.; Pompei, R.; Bonsignore, L. Antimicrobial evaluation of coumarins and flavonoids from the stems of *Daphne gnidium* L. *Phytomedicine* **2001**, *8*, 302-305, <https://doi.org/10.1078/0944-7113-00036>.
19. Kumar, A.; Sunita, P.; Jha, S.; Pattanayak, S.P. Daphnetin inhibits TNF- $\alpha$  and VEGF-induced angiogenesis through inhibition of the IKKs/I $\kappa$ B $\alpha$ /NF- $\kappa$ B, Src/FAK/ERK1/2 and Akt signalling pathways. *Clin. Exp. Pharmacol. Physiol.* **2016**, *43*, 939-950, <https://doi.org/10.1111/1440-1681.12608>.
20. Singh, L.; Singh, A.P.; Bhatti, R. Mechanistic interplay of various mediators involved in mediating the neuroprotective effect of daphnetin. *Pharmacol Rep.* **2021**, *73*, 1220-1229, <https://doi.org/10.1007/s43440-021-00261-z>.
21. Lv, H.; Fan, X.; Wang, L.; Feng, H.; Ci, X. Daphnetin alleviates lipopolysaccharide/D-galactosamine-induced acute liver failure *via* the inhibition of NLRP3, MAPK and NF- $\kappa$ B, and the induction of autophagy. *Int. J. Biol. Macromol.* **2018**, *119*, 240-248, <https://doi.org/10.1016/j.ijbiomac.2018.07.101>.
22. Zhang, L.; Gu, Y.; Li, H.; Cao, H.; Liu, B.; Zhang, H.; Shao, F. Daphnetin protects against cisplatin-induced nephrotoxicity by inhibiting inflammatory and oxidative response. *Int. Immunopharmacol.* **2018**, *65*, 402-407, <https://doi.org/10.1016/j.intimp.2018.10.018>.
23. Song, B.; Wang, Z.; Liu, Y.; Xu, S.; Huang, G.; Xiong, Y.; Zhang, S.; Xu, L.; Deng, X.; Guan, S. Immunosuppressive Activity of Daphnetin, One of Coumarin Derivatives, Is Mediated through Suppression of NF- $\kappa$ B and NFAT Signaling Pathways in Mouse T Cells. *PLOS ONE* **2014**, *9*, e96502, <https://doi.org/10.1371/journal.pone.0096502>.
24. Wróblewska-Łuczka, P.; Góralczyk, A.; Łuszczki, J.J. Daphnetin, a Coumarin with Anticancer Potential against Human Melanoma: *In vitro* Study of Its Effective Combination with Selected Cytostatic Drugs. *Cells* **2023**, *12*, 1593, <https://doi.org/10.3390/cells12121593>.
25. Pangal, A.; Ahmed, K. Synthesis, Biological Evaluation and Molecular Docking Studies of C-3 Substituted Coumarin Analogs to Explore their Anti-Proliferative Potential. *Curr. Trends Biotechnol. Pharm.* **2023**, *17*, 649-659, <https://doi.org/10.5530/ctbp.2023.1.6>.
26. Pangal, A.; Shaikh, J.A.; Mulani, M.; Ahmed, K. Synthesis, anticancer activities and *in silico* screening of 3-acetylcoumarin hydrazone scaffolds. *J. Adv. Sci. Res.* **2021**, *12*, 225-233, <https://doi.org/10.55218/JASR.s1202112425>.
27. Isyaku, Y.; Uzairu, A.; Uba, S. Computational studies of a series of 2-substituted phenyl-2-oxo-, 2-hydroxyl- and 2-acyloxyethylsulfonamides as potent anti-fungal agents. *Heliyon* **2020**, *6*, e03724, <https://doi.org/10.1016/j.heliyon.2020.e03724>.
28. Nisha, C.M.; Kumar, A.; Nair, P.; Gupta, N.; Silakari, C.; Tripathi, T.; Kumar, A. Molecular Docking and *In Silico* ADMET Study Reveals Acylguanidine 7a as a Potential Inhibitor of  $\beta$ -Secretase. *Adv. Biotechnol.* **2016**, *2016*, 9258578, <https://doi.org/10.1155/2016/9258578>.
29. Żółek, T.; Maciejewska, D. Theoretical evaluation of ADMET properties for coumarin derivatives as compounds with therapeutic potential. *Eur. J. Pharm. Sci.* **2017**, *109*, 486-502, <https://doi.org/10.1016/j.ejps.2017.08.036>.
30. Pangal, A.; Tambe, P.; Ahmed, K. Screening of 3-acetylcoumarin derivatives as multifunctional biological agents. *Cur. Chem. Lett.* **2023**, *12*, 343-352, <http://dx.doi.org/10.5267/j.ccl.2022.12.005>.
31. Pangal, A.; Mujahid, Y.; Desai, B.; Shaikh, J.A.; Ahmed, K. Synthesis of 3-(2-(substituted-(trifluoromethyl)-phenylamino)acetyl)-2H-chromen-2-one derivatives as new anticancer agents. *Cur. Chem. Lett.* **2022**, *11*, 105-112, <https://doi.org/10.5267/j.ccl.2021.8.004>.

32. Pangal, A.; Ahmed, K. Synthesis and biological evaluation of coumarin-quinone hybrids as multifunctional bioactive agents. *ADMET DMPK*. **2022**, *11*, 81-96, <https://doi.org/10.5599%2Fadmet.1468>.
33. Shaikh, S.B.; Tambe, P.; Mujahid, Y.; Santra, M.K.; Biersack, B.; Ahmed, K. Targeting growth of breast cancer cell line (MCF-7) with curcumin-pyrimidine analogs. *J. Chem. Sci.* **2022**, *134*, 123, <https://doi.org/10.1007/s12039-022-02115-4>.
34. Jiang, Y.-L.; Tang, L.-Q.; Miyanaga, S.; Igarashi, Y.; Saiki, I.; Liu, Z.-P. Synthesis and evaluation of trehalose-based compounds as anti-invasive agents. *Bioorg. Med. Chem. Lett.* **2011**, *21*, 1089-1091, <https://doi.org/10.1016/j.bmcl.2010.12.133>.
35. Shaikh, J.; Pangal, A.; Tamboli, I.; Pote, G.; Ahmed, K. Design and *in silico* evaluation of new azobarbituric acid analogs as possible anticancer agents. *Heterocycl. Lett.* **2022**, *12*, 725-735, <https://doi.org/10.6084/m9.figshare.21647096.v2>.